Investigation of the Effects of Isotopic Labeling at a PS/PMMA Interface Using SIMS and Mean-Field Theory

Shane E. Harton,[†] Frederick A. Stevie,[‡] and Harald Ade*[,§]

Department of Materials Science & Engineering, North Carolina State University, Raleigh, North Carolina 27695; Analytical Instrumentation Facility, North Carolina State University, Raleigh, North Carolina 27695; and Department of Physics, North Carolina State University, Raleigh, North Carolina 27695

Received October 14, 2005; Revised Manuscript Received December 4, 2005

ABSTRACT: Isotopic labeling (deuteration) is known to affect the phase behavior of polystyrene (PS) and poly(methyl methacrylate) (PMMA) blends, but little is known regarding the changes in the interfacial properties at the PS/PMMA interface due to deuteration of PS and/or PMMA. To investigate these potential changes, secondary ion mass spectrometry (SIMS) was used to measure real-space depth profiles of dPS in hPS:dPS/hPMMA bilayers, with the hPS:dPS blend being well within the single-phase region of the phase diagram. Profound changes in the thermodynamic behavior of this system at the polymer/polymer interface are observed in the form of significant segregation of dPS to the hPS:dPS/hPMMA interface. The observation of a depletion hole during the formation of an equilibrium excess of dPS implies that the energetic gain at the interface per dPS chain has to be $>kT$. These results cannot be described, even qualitatively, using previously reported changes in χ for PS/PMMA due to isotopic labeling. The previously reported values of χ for dPS/hPMMA and hPS/hPMMA actually predict a depletion of dPS at the hPS:dPS/hPMMA interface rather than the observed segregation. The observed interfacial excess is quantified by generating theoretical profiles, using self-consistent mean-field theory (SCMF), and fitting an effective interaction energy parameter $\Delta\chi_p$ as a function of temperature. This parameter represents the asymmetry in dPS/hPMMA and hPS/PMMA interactions. The temperature dependency of $\Delta\chi_p$ was found to be a factor of 3−4 greater than any of those reported for χ of PS/PMMA. It was also found that SCMF theory accurately describes the concentration dependency of dPS segregation at a constant dPS molecular weight using a concentration-independent $\Delta\chi_p$; however, $\Delta\chi_p$ was found to be dependent on dPS molecular weight.

Introduction

Isotopic labeling of polymers is a well-established method for providing a tracer component or creating enhanced contrast for characterization using experimental techniques such as small-angle neutron scattering (SANS),[1] neutron specular reflectivity (NR),[2] forward recoil spectrometry (FRES),[3] and secondary ion mass spectrometry (SIMS).[4,5] Although labeling is often necessary for experimental characterization, it is well-known that deuterium labeling (deuteration) can alter the thermodynamic properties of the polymer constituents.[6−8] In fact, many simple mixtures involving a polymer species and its deuterated analogue are known to have a small, but finite, mean-field interaction parameter χ and are characterized by upper-critical solution-type phase behavior (UCST).[7,9,10] Therefore, a polymer mixture of hA and dA, where hA is unlabeled polymer A and dA is deuterium-substituted polymer A, can exhibit classical phase changes such as spinodal decomposition.[11]

The effects of deuteration can also influence the surface and interfacial interactions of polymers. Deuterium-substituted polystyrene (dPS) is known to have a lower surface tension than simple hydrogen-containing PS (hPS),[12] and it has an enthalpic preference for a silicon oxide (SiOx) surface.[13] These types of interactions have been shown to be significant at conditions well within the single-phase region of the phase diagram. Even with the enormous amount of existing information on the effects of isotopic labeling, investigations involving the effects of deuteration at polymer/polymer interfaces have been limited.[14] Here, we probe the effects of deuteration at a polymer/polymer interface using secondary ion mass spectrometry (SIMS) and a highly investigated polymer pair, PS and poly(methyl methacrylate) (PMMA).[15−17] Results show significant changes in the thermodynamic behavior of this system at the polymer/polymer interface, namely significant segregation of dPS to the hPS:dPS/hPMMA interface. Control experiments with end-functional polymers eliminated segregation due to end groups as a possible reason for the observed segregation. A mean-field theory[18,19] that was previously implemented to describe surface segregation of dPS and segregation of dPS to an hPS:dPS/SiOx interface[13,20] is used to quantify the results presented here for segregation of dPS to an hPS:dPS/hPMMA interface as a function of temperature, dPS concentration, and dPS molecular weight. An energetic parameter $\Delta\chi_p$, which is related to the difference in χ for dPS/hPMMA and hPS/PMMA, was determined as a function of temperature. It is clearly shown that the results presented here cannot be described, even qualitatively, using the reported changes in χ for PS/PMMA due to isotopic labeling.[6]

Experimental Section

Atactic PS (hPS and dPS), syndiotactic hPMMA, and atactic poly(2-vinylpyridine) (hP2VP) were purchased from Polymer Source (PolS) or Scientific Polymer Products (SPP). Their molecular weight and polydispersity properties are listed in Table 1. All dPS have ≈100% deuterium substitution (perdeuterated). The inflection-point glass transition temperatures (T_g's) of the respective polymers, as determined using DSC (10 °C/min cooling cycle), are also listed in Table 1. Silicon (100) substrates were cut to 2.5 cm × 2.5 cm squares and cleaned according to established procedures.[21] First, the substrates were soaked in a sulfuric acid/hydrogen peroxide/

[†] Department of Materials Science & Engineering.
[‡] Analytical Instrumentation Facility.
[§] Department of Physics.
* Corresponding author: e-mail harald_ade@ncsu.edu.

10.1021/ma052236z CCC: $33.50
Published on Web 01/26/2006

Table 1. Polymers Used in This Investigation

polymer	T_g/°C	supplier	M_w/kDa	M_w/M_n
dPS-130	97	PolS	140	1.07
dPS-70	97	PolS	82.8	1.15
hPS-130	96	PolS	138	1.05
hPS-70	96	PolS	73.0	1.04
hPMMA	127	PolS	155	1.05
hP2VP	98	SPP	514	1.08
dPS-OH	97	PolS	76.6	1.05

Table 2. Sample Properties for Various Systems Employed[a]

system	PS layer	h_{PS}/nm	bottom layer
A	5% dPS-130 + 95% hPS-130	255	hPMMA
B	5% dPS-130 + 95% hPS-130	230	hPMMA
C	10% dPS-130 + 90% hPS-130	250	hPMMA
D	20% dPS-130 + 80% hPS-130	240	hPMMA
E	30% dPS-130 + 70% hPS-130	225	hPMMA
F	10% dPS-70 + 90% hPS-70	210	hPMMA
G	10% dPS−OH + 90% hPS-70	170	hP2VP
H	100% dPS-130	100	hPMMA

[a] For systems A−G the bottom layer (hPMMA or hP2VP) was ≈200 nm, while the hPMMA layer thickness was 100 nm for system H. Concentrations (% v/v) are based on volume fraction at $t = 0$.

water (1:1:3) bath at 100 °C for 30 min to remove organic and inorganic contaminants and then washed with deionized water. Then, they were soaked in aqueous HF (∼10% v/v) for 1 min, washed with deionized water, and blown dry with nitrogen leaving a hydrogen-passivated substrate (SiH). hPMMA and hP2VP were spun-cast from chlorobenzene onto SiH to a thickness ≈200 nm and annealed at 150 °C for 3 h. PS (hPS + dPS) was cast directly onto hPMMA or hP2VP from 1-chloropentane, a selective solvent for PS over PMMA or P2VP.[17] For segregation measurements, the PS thickness ranged from ≈200−250 nm, and the dPS concentration was varied from 5 to 30% (v/v) relative to the total PS. Samples were annealed under vacuum at temperatures ranging from 128 to 166 °C. A bilayer consisting of 100 nm 100% dPS-130 on 100 nm hPMMA was also prepared to quantify sputtering rates and the depth resolution during SIMS analysis. All systems are listed in Table 2.

The deuterium depth profiles were acquired using a CAMECA IMS-6f magnetic sector spectrometer. Typical conditions implemented for the PS/PMMA system involved a 25−30 nA O_2^+ primary beam with 5.5 keV impact energy that was rastered over a 180 μm × 180 μm area. Positive secondary ions were detected from a 60 μm diameter optically gated area at the center of the raster crater. A mass resolution ($m/\Delta m$) of 1250 was used to completely separate D^+ from H_2^+ while maintaining high detection sensitivity.[17,22] For the hPS:dPS-OH/hP2VP system, identical conditions were used with the exception of a 50 nA O_2^+ primary ion beam. Before the bilayers were analyzed, a 50 nm hPS sacrificial layer was added to the sample surface to ensure uniform sputtering rates and secondary ion yields before the start of the hPS:dPS layer. A 20 nm Au coating was deposited on top of the sacrificial layer to prevent charge buildup. Three to four spots on each sample were analyzed.

Results and Discussion

From Figure 1, it is clearly evident that dPS preferentially segregates to the hPS:dPS/hPMMA interface at 128 °C. The depletion hole at the hPS:dPS surface and hPS:dPS/hPMMA interfaces (Figure 1b) after 4 h (system B) indicates that this is a diffusion-controlled event. Diffusion-controlled segregation of dPS to an hPS:dPS surface has been quantified previously, although without direct observation of a depletion hole.[12,23] However, this phenomenon has not been observed for homopolymer segregation to a polymer/polymer interface. The observation of the depletion hole implies that the energetic gain at the interface per dPS chain has to be $> kT$, which is

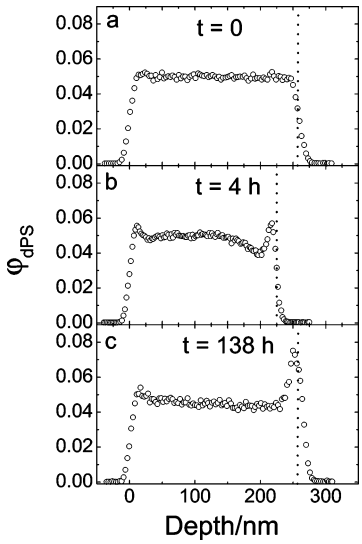

Figure 1. SIMS profiles for the dPS-130 volume fraction (φ_{dPS}) as a function of depth after annealing at 128 °C for (a) 0 (system A, 255 nm thick), (b) 4 h (system B, 230 nm thick), and (c) 138 h (system A, 255 nm thick). A clear depletion hole with a corresponding interfacial excess is apparent near the dPS:hPS/PMMA interface after 4 h (b). A large segregated amount of dPS-130 is present after 138 h (c). The interfaces are marked here and in similar subsequent figures by a line as a visual quide to the approximate (dPS:hPS)/PMMA interface location.

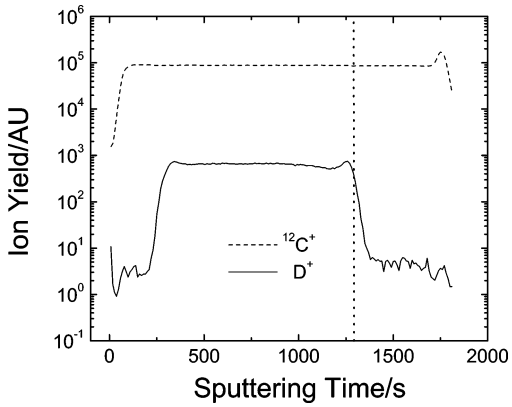

Figure 2. Raw SIMS profiles (i.e., secondary ion yield as a function of sputtering time) for D^+ and the $^{12}C^+$ matrix after 4 h at 128 °C (system B). A constant $^{12}C^+$ secondary ion yield is observed through the hPS:dPS/hPMMA interface (vertical line), clearly demonstrating that the profiles shown in Figure 1 are not analysis artifacts.

surprisingly large. At longer times (Figure 1c) there is a considerable amount of dPS at the hPS:dPS/hPMMA interface (system A). Figure 2 shows the raw SIMS profiles for D^+ and the $^{12}C^+$ matrix after 4 h at 128 °C (system B). The use of O_2^+ primary ion bombardment with detection of positive primary ions, under the conditions implemented here, provides a constant $^{12}C^+$ secondary ion yield through the hPS:dPS/hPMMA interface, which has been observed previously.[24] This is an optimal situation for analysis of a heterogeneous interface, and it should be noted that these analysis conditions (i.e., detection of positive secondary ions) could not be implemented with the commonly used quadrupole SIMS instrument, with its inferior mass resolution (typical $m/\Delta m \sim 300$) and, hence, inability to mass resolve D^+ from H_2^+.[4,25] Therefore, the phenomena observed at the hPS:dPS/hPMMA interface in Figure 1b,c are not artifacts of the SIMS analysis. This is also evidenced in Figure 1a with the absence of any discernible features near the hPS:dPS/hPMMA interface for $t = 0$.

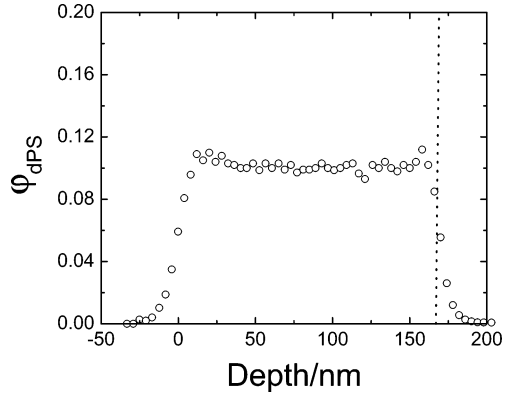

Figure 3. SIMS depth profile of system G after 96 h at 130 °C. Because an −OH group, such as that at the end of the dPS-OH is known to hydrogen bond with P2VP much more strongly than with PMMA the negligible dPS-OH excess at the hPS:dPS-OH/P2VP interface (vertical line) further supports that unwanted end-functional groups on the dPS-130 are not the underlying cause of the dPS segregation shown in Figure 1.

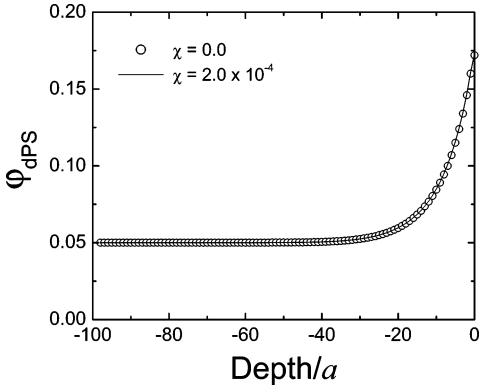

Figure 4. SCMF-L results for $N_{dPS} = N_{hPS} = 1200$, $\Delta\chi_p = 0.01$, and χ for hPS:dPS = 0.0 (○) and 2.0×10^{-4} (solid line). The interface is set to 0, and the depth is scaled to the statistical segment length (a) of hPS and dPS. At these molecular weights, the hPS:dPS interaction is completely negligible.

To ensure that the observed segregation of dPS is not driven by chemical bonding or specific interactions due to unwanted functional groups created on the dPS by improper synthesis,[26] a control experiment was performed with a system containing highly end-functionalized dPS (dPS-OH; >95% −OH end-functionalized) and P2VP as bottom layer. P2VP was chosen because it does not show strong isotopically driven segregation. It has the added benefit of having an enhanced attractive enthalpic interaction of the −OH end group at the interface, as it was previously determined that an −OH moiety will hydrogen bond much more strongly with the tertiary amine groups in the P2VP than the carbonyl groups in PMMA.[27] After 96 h at 130 °C, there is negligible interfacial segregation of dPS-OH to the hPS:dPS-OH/hP2VP interface, as shown in Figure 3. Another common end-functional group such as −COOH (carboxy) would be expected to behave in a similar manner. Therefore, end groups that might have been unintentionally introduced to the dPS-130 (primarily −COOH from carbon dioxide contamination[28]) would not play a significant role in the interfacial segregation of dPS at a hPS:dPS/hPMMA interface. A functional group such as a primary amine, which is highly unlikely to be unintentionally introduced, would be required to irreversibly react with the ester groups along the PMMA chain to cause an interfacial excess.[29]

For quantitative analysis of the interfacial segregation, we have employed a self-consistent mean-field lattice model (SCMF-L)[18] as derived previously for polymer segregation to polymer surfaces and polymer/substrate interfaces.[19] A cubic lattice was used for all calculations. Because the relaxed chain diameter of dPS-130 ($R_0 = aN^{1/2} \approx 23$ nm, where R_0 is the rms end-to-end distance, a is the statistical segment length, and N is the number of segments in a dPS-130 chain) is much greater than the overlap of PS and PMMA at the interface ($w_{1/2} = a/(6\chi)^{1/2} \approx 1.4$ nm for $\chi = 0.038$),[16,30] the PMMA layer is treated as an infinitely flat (rigid) substrate. The free energy of mixing (F_M) in the hPS:dPS layer can be described using the Flory−Huggins expression[31]

$$\frac{F_M}{kT} = \frac{n_{dPS}}{N_{dPS}} \ln \varphi_{dPS} + \frac{n_{hPS}}{N_{hPS}} \ln \varphi_{hPS} + \chi_{dPS,hPS} n_{dPS} \varphi_{hPS} \quad (1)$$

where n_{dPS} and n_{hPS} are the number of segments of dPS and hPS, respectively. When the constraints of a surface are imposed, an excess energy is incorporated:

$$\frac{F_s}{kT} = -\Delta\chi_s n'_{dPS} \quad (2)$$

where n'_{dPS} is the number of dPS segments in contact with the surface, and $kT\Delta\chi_s$ is the net energetic preference for dPS over hPS at a surface.[13,19,20] Similarly

$$\frac{F_p}{kT} \equiv -\Delta\chi_p n'_{dPS} = \lambda_1(\chi_{dPS,hPMMA} - \chi_{hPS,hPMMA}) n'_{dPS} \quad (3)$$

where $kT\Delta\chi_p$ is the net energetic preference per segment for dPS over hPS at an hPMMA "substrate", and λ_1 is a lattice weighting factor (1/6 for cubic).[18] As shown in eq 3, $\Delta\chi_p$ should be proportional to a simple difference in χ values for dPS/hPMMA and hPS/hPMMA. Realistically, we would expect the number of contacts between PS (hPS or dPS) and hPMMA to be greater than one per segment, as there is indeed finite overlap at the interface. Therefore, $\Delta\chi_p$ can be considered an effective fitting parameter with physical limits

$$1 \geq \frac{\Delta\chi_p}{\chi_{hPS,hPMMA} - \chi_{dPS,hPMMA}} \geq \lambda_1 \quad (4)$$

The use of this model helps to minimize computational cost, and it allows for direct comparison to parameters that have been previously determined for dPS segregation to hPS:dPS surfaces and hPS:dPS/SiOx interfaces.[13,20]

The reported χ values for hPS:dPS are nominally 2.0×10^{-4} over the range of temperatures employed in this investigation (128−166 °C).[10,32] Figure 4 shows a theoretical comparison of dPS segregation using $\chi = 0.0$ and $\chi = 2.0 \times 10^{-4}$ for $N_{hPS} = N_{dPS} = 1200$ and $\Delta\chi_p = 0.01$. For the molecular weights used here, the interaction between hPS and dPS is negligible, as the system is deep inside the single-phase region of the phase diagram ($\chi N \ll 2$). Therefore, segregation of dPS-130 to the interface is driven exclusively by the $-kT\Delta\chi_p$ energy gain, and as such, it can be assumed that $\chi \approx 0.0$ for the hPS:dPS blends used here.

PS and PMMA are known to have a weak enthalpic interaction with each other, with or without isotopic labeling (see Table 3).[6,33] The temperature dependency of the dPS segregation was tested for system B at temperatures ranging

Table 3. Values of χ for PS/PMMA as a Function of Isotopic Labeling As Previously Reported in Ref 6[a]

polymer pair	$\chi(T)$
hPS/hPMMA	$3.20/T + 0.021$
dPS/hPMMA	$3.902/T + 0.0284$
hPS/dPMMA	$3.188/T + 0.0292$
dPS/dPMMA	$3.199/T + 0.0251$

[a] Note that χ for dPS/hPMMA, hPS/dPMMA, and dPS/dPMMA were measured with block copolymers using SANS in refs 6 and 39, and χ for hPS/hPMMA originated from cloud point measurements of homopolymers in ref 33.

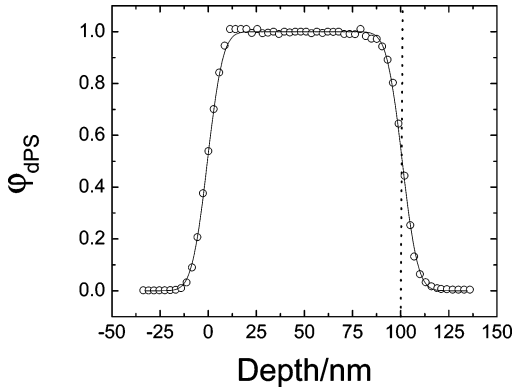

Figure 5. SIMS depth profile of system H (100% dPS-130), which was used to quantify the depth resolution. From a Gaussian convoluted step function (error function) the effective depth resolution was determined to be 15 nm (FWHM).

from 138 to 166 °C by fitting convoluted theoretical profiles to SIMS depth profiles. A constant value of $\Delta\chi_s = 0.005$, as reported previously for dPS surface segregation at 160 °C,[20] was used to account for dPS segregation to the hPS:dPS surface. To determine the effective depth resolution, system H was fit to a Gaussian convoluted step function (error function) with a measured full width at half-maximum (FWHM) of 15 nm, as shown in Figure 5. Besides the inherent instrumental convolution for a given system and analysis conditions,[22,34] any convolution due to interfacial roughness[35] is also included in this value.[36] This line shape represents the profile quite well, at both the sacrificial layer/dPS and dPS/hPMMA interfaces, and as such, Gaussian convolution with a constant FWHM = 15 nm was used to convolute the theoretical depth profiles.

Figure 6 shows the depth profiles and convoluted SCMF-L profiles for system B. Three to four different profiles at each condition were analyzed. For system A, no change in the dPS profile was found after annealing for times greater than 94 h at 138 °C. Tracer diffusion coefficients ($D°$)[37] and characteristic diffusion times[38] ($\tau_D = L^2/4D°$, where L is the PS layer thickness) for dPS-130 are shown in Table 4. According to the relative diffusion times ($\tau_D/\tau_{D,138}$) shown in Table 4, all annealing times used here were sufficient to reach equilibrium segregation, with the exception of the profiles shown in Figure 1. Qualitatively, one can see a clear decrease in the interfacial segregation of dPS from 138 to 166 °C. The quantitative changes in the interfacial interactions from 138 to 166 °C are shown in Figure 7, with a comparison to the values of $\Delta\chi_p$ measured here and the reported values of χ for hPS/hPMMA, dPS/dPMMA, dPS/hPMMA, and hPS/dPMMA (see Table 3).[6,33] The values for hPS/hPMMA had been determined using cloud-point measurements with homopolymer mixtures,[33] while the values for the dPS/dPMMA, dPS/hPMMA, and hPS/dPMMA had been determined using SANS of block copolymers.[6,39] The rms error for the $\Delta\chi_p$ measurements is approximately 2−3% for all

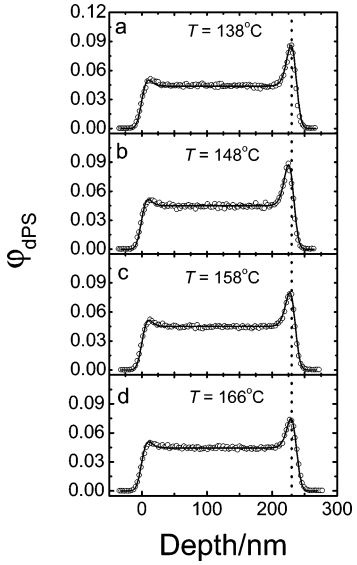

Figure 6. SIMS depth profiles for 5% (v/v) initial dPS-130 concentration (○) compared to convoluted theoretical profiles generated using SCMF-L (solid lines) for system B after (a) 160 h at 138 °C, (b) 73 h at 148 °C, (c) 53 h at 158 °C, and (d) 41 h at 166 °C. The values of $\Delta\chi_p$ were determined by fitting theoretical profiles to the experimental profiles at each temperature. The PS/PMMA interface is shown with the vertical line.

Table 4. Tracer Diffusion Coefficients ($D°$) for dPS-130 from Ref 37 and Characteristic Diffusion Times ($\tau_D = L^2/4D°$, Where L Is the PS Layer Thickness) for dPS-130[a]

T/°C	$D°$/(nm²/s)	τ_D/h	$\tau_D/\tau_{D,138}$
138	0.26	16.7	1.00
148	1.22	3.5	0.21
158	4.86	0.89	0.05
166	13.3	0.33	0.02

[a] A constant $L = 250$ nm was assumed.

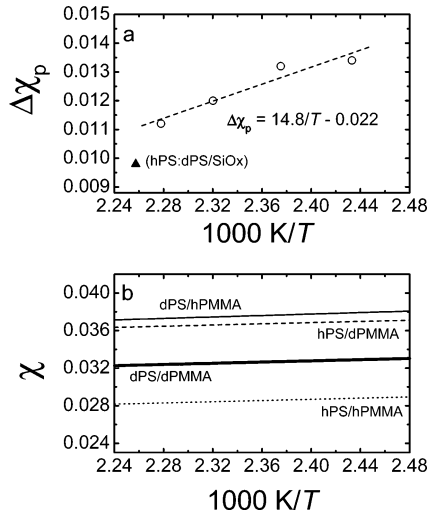

Figure 7. A comparison of (a) values of $\Delta\chi_p$ determined from Figure 6 (○) with the linear regression (dashed line) and (b) χ reported in ref 6 for dPS/hPMMA (solid line), hPS/dPMMA (dashed line), dPS/dPMMA (bold line), and hPS/hPMMA (dotted line) (see Table 3). The temperature dependency for (a) $\Delta\chi_p$ is a factor of 3−4 greater than those for (b) χ. Also shown in (a) is the value for $\Delta\chi_s$ for hPS:dPS/SiOx at 170 °C (▲) from ref 12.

values shown in Figure 7a. According to the linear fit of $\Delta\chi_p$ vs $1/T$ (see Figure 7a)

$$\Delta\chi_p = \frac{14.8}{T} - 0.022 \qquad (5)$$

CDV

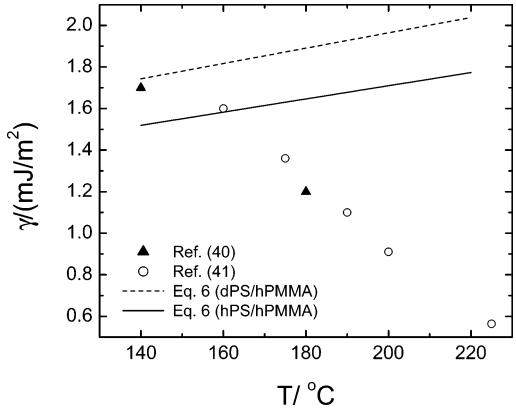

Figure 8. Interfacial tension (γ) measurements for hPS/hPMMA from refs 40 (▲) and 41 (○) as compared to values predicted by mean-field theory (eq 6) using values of χ for (dashed line) dPS/hPMMA and (solid line) hPS/hPMMA from ref 6.

the reported values of χ for dPS/hPMMA and hPS/hPMMA actually predict a *depletion* of dPS at the hPS:dPS/hPMMA interface ($\Delta\chi_p < 0$) rather than the observed *segregation*, and the temperature dependency of $\Delta\chi_p$ in eq 5 is a factor of 3−4 greater than any of the values shown in Table 3. In fact, the reported change in χ for PS/PMMA over the temperature range used here (128−166 °C) is very small for all the values shown in Figure 7b, and the temperature dependence of $\Delta\chi_p$ using reported values would be completely negligible. This type of discrepancy can also be observed with interfacial tension (γ) measurements for hPS/hPMMA[40,41] when compared to γ predicted by the mean-field expression[30]

$$\gamma = a\rho_0 kT\left(\frac{\chi}{6}\right)^{1/2} \tag{6}$$

where ρ_0 is the segmental density[16] (5.75 nm^{-3}). As shown in Figure 8, mean-field theory does not even qualitatively describe γ for hPS/hPMMA when the values for χ determined from bulk systems are used. The mechanism behind this apparent change in the phase behavior of PS/PMMA from bulk miscible systems to heterogeneous systems (interface) is not understood at this time.

The $\Delta\chi_s$ reported for dPS segregation to a hPS:dPS/SiOx interface at 170 °C ($\Delta\chi_s = 0.0098$)[13] is also shown in Figure 7a. Clearly, the effects of isotopic labeling are more pronounced at an hPS:dPS/hPMMA than the hPS:dPS/SiOx interface, which is further demonstrated with a comparison of the theoretical dPS excess (Z^*) for segregation of dPS to a hPS:dPS/SiOx interface, hPS:dPS/hPMMA interface, and an hPS:dPS surface ($\Delta\chi_s = 0.005$)[20] for $N_{dPS} = N_{hPS} = 1200$, as shown in Figure 9. The excess was calculated from

$$\frac{Z^*}{a} \equiv \int_{M_1}^{M_2} (\varphi_{dPS} - \varphi_{dPS,b})\, dz' \tag{7}$$

where z' is the depth scaled to the statistical segment length (a), M_1 is the (scaled) depth where φ_{dPS} becomes $\varphi_{dPS,b}$ (bulk concentration of dPS), and M_2 is the location of the interface (or surface), and scaled to the dPS radius of gyration ($R_g = a(N/6)^{1/2} \approx 9.5$ nm). Because the SCMF-L model is inherently discrete,[18] eq 7 becomes a simple summation.

Next, the ability of the SCMF-L model to describe the dPS segregation as a function of dPS concentration and dPS molecular weight is evaluated. All of the systems employed for this (systems C−F) were brought to equilibrium at 138 °C, and constant values of $\Delta\chi_p = 0.0134$ and $\Delta\chi_s = 0.005$ were used

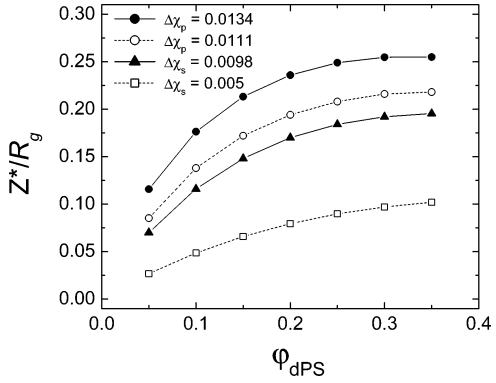

Figure 9. Comparison of normalized interfacial excess (Z^*/R_g), calculated from SCMF-L and eq 7 and scaled to the dPS-130 R_g (≈9.5 nm), as a function of dPS concentration for (●) $\Delta\chi_p = 0.0134$ (hPS:dPS/hPMMA interface at 138 °C), (○) $\Delta\chi_p = 0.0111$ (extrapolation from Figure 7) (hPS:dPS/hPMMA interface at 170 °C), (▲) $\Delta\chi_s = 0.0098$ (hPS:dPS/SiOx interface at 170 °C), and (□) $\Delta\chi_s = 0.005$ (hPS:dPS surface at 160 °C). Lines are a guide for the eye. Clearly, dPS segregates much more strongly to an hPS:dPS/hPMMA interface than an hPS:dPS/SiOx interface or an hPS:dPS surface.

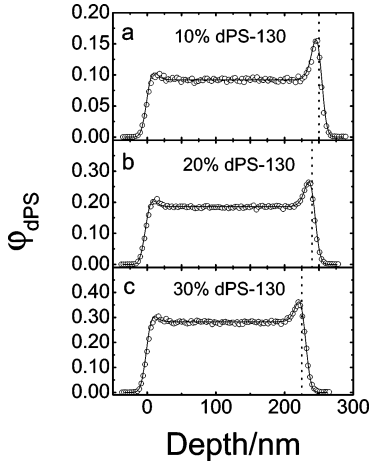

Figure 10. SIMS depth profiles (○) for dPS-130 segregation after 94 h at 138 °C for initial concentrations of (a) 10% dPS (system C), (b) 20% dPS (system D), and (c) 30% dPS (system E). The PS/PMMA interface is shown with the vertical line. The convoluted theoretical profiles (solid line) were generated using a constant value of $\Delta\chi_p = 0.0134$. Excellent agreement is found with a constant $\Delta\chi_p$ over this concentration range for dPS-130 segregation at 138 °C.

for all calculations. Clearly the SCMF-L model provides excellent representation of the dPS-130 segregation at 138 °C for 10−30% (v/v) dPS using the constant value of $\Delta\chi_p$. The excellent agreement of the concentration dependence indicates that the model does indeed provide some physical interpretation of the isotopically driven segregation for systems A−E. Values for Z^*/R_g as a function of dPS concentration at 138 °C are shown in Figure 10. To determine whether the model is truly universal for dPS segregation to an hPS:dPS/hPMMA interface, system F (10% dPS-70 + 90% hPS-70) was analyzed after equilibration at 138 °C. After comparison to the SCMF-L model (see Figure 11), it is evident that the model does not quantitatively describe the molecular weight dependency. A value of $\Delta\chi_p \approx 0.016$ provides much better theoretical agreement with the experimental results for dPS-70 segregation at 138 °C.

An apparent change in the energetic interaction with molecular weight has been observed previously with surface segregation of dPS.[20] The value of $\Delta\chi_s$ for an hPS:dPS surface was shown to deviate by as much as 50% from the nominal value of 0.005 over a range of dPS molecular weights of ∼30−500

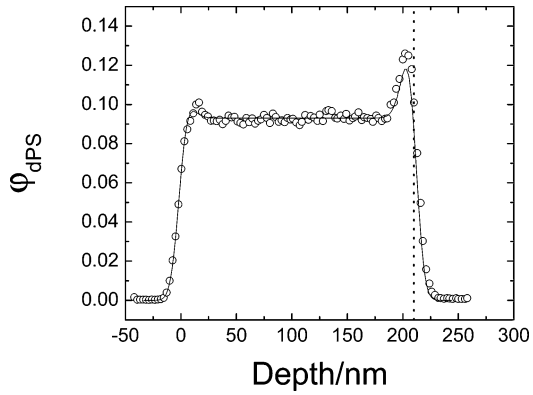

Figure 11. SIMS depth profiles (○) for dPS-70 segregation after 94 h at 138 °C for an initial concentration of 10% dPS (system F). The PS/PMMA interface is shown with the vertical line. The convoluted theoretical profile (solid line) was generated using a value of $\Delta\chi_p = 0.0134$, which was measured with system B (dPS-130) at this temperature. The SCMF-L theory does not appear to accurately predict the changes in dPS segregation as a function of molecular weight with a constant $\Delta\chi_p$. A $\Delta\chi_p \approx 0.016$ would be required to represent the profile shown here.

kDa.[20] This is also evidenced in Figure 11 with the surface excess of dPS-70, which is clearly larger for the measured profile than the simulated profile using $\Delta\chi_s = 0.005$. Therefore, there is an apparent increase in $\Delta\chi_p$ and $\Delta\chi_s$ from dPS-130 to dPS-70. Finite overlapping of PS and PMMA at the interface may be the reason behind the change in $\Delta\chi_p$. This could also be the result of an inability of the Flory−Huggins theory to accurately describe the entropic changes in the system. Modifications have been made to this theory through incorporation of equation-of-state effects.[42] These effects were shown to be particularly important for dPS segregation to an hPS:dPS surface when dPS and hPS have significantly different chain lengths (molecular weights).[43,44] Because χ for PS/PMMA (bulk) is nearly independent of temperature, owing primarily to entropic contributions,[6,33] incorporation of equation-of-state effects may be necessary for a more complete theoretical description of this system.

Conclusions

The effects of isotopic labeling have been shown experimentally to have profound effects at a PS/PMMA interface. dPS was observed to strongly segregate to an hPS:dPS/hPMMA interface from a symmetric dPS:hPS blend with dPS concentrations ranging from 5 to 30% (v/v) and temperatures ranging from 128 to 166 °C. At 128 °C, diffusion-controlled segregation was observed (see Figure 1), implying an energetic gain $> kT$ per dPS chain. Using a self-consistent mean-field lattice model,[18,19] the enthalpic preference for dPS over hPS at the hPS:dPS/hPMMA interface was interpreted using an energetic parameter $\Delta\chi_p$. These results are in complete disagreement with previously reported χ values for PS/PMMA as a function of isotopic labeling (see Figure 7b),[6] which predict a depletion of dPS at a hPS:dPS/hPMMA interface. The temperature dependency is much greater for $\Delta\chi_p$ (see Figure 7a) than for any of the reported values of χ for PS/PMMA (see Table 3 and Figure 7b). Analogously, the reported values for the interfacial tension γ of PS/PMMA show a strong decrease with increasing temperature; however, the reported values of χ predict an increase in γ with increasing temperature (see Figure 8). This indicates an apparent change in the in phase behavior of PS/PMMA from bulk miscible systems to heterogeneous systems (interface). Although SCMF-L could accurately describe the concentration dependence for dPS-130 segregation at 138 °C using a single value of $\Delta\chi_p = 0.0134$, universal behavior was not found when the molecular weight was varied.

Acknowledgment. The authors gratefully acknowledge invaluable discussions with Prof. M. Rubinstein (University of North Carolina) and Prof. S. Kumar (Rensselaer Polytechnic Institute). This work was supported by the U.S. Department of Energy (DE-FG02-98ER45737).

References and Notes

(1) Roe, R.-J. *Methods of X-Ray and Neutron Scattering in Polymer Science*; Oxford University Press: New York, 2000.
(2) Zhao, W.; Zhao, X.; Rafailovich, M. H.; Sokolov, J.; Mansfield, T.; Stein, R. S.; Composto, R. C.; Kramer, E. J.; Jones, R. A. L.; Sansone, M.; Nelson, M. *Physica B* **1991**, *173*, 43.
(3) Composto, R. J.; Walters, R. M.; Genzer, J. *Mater. Sci. Eng., R* **2002**, *38*, 107.
(4) Schwarz, S. A.; Wilkens, B. J.; Pudensi, M. A. A.; Rafailovich, M. H.; Sokolov, J.; Zhao, X.; Zhao, W.; Zheng, X.; Russell, T. P.; Jones, R. A. L. *Mol. Phys.* **1992**, *76*, 937.
(5) Harton, S. E.; Stevie, F. A.; Ade, H. *J. Vac. Sci. Technol. B*, submitted for publication.
(6) Russell, T. P. *Macromolecules* **1993**, *26*, 5819.
(7) Bates, F. S.; Muthukumar, M.; Wignall, G. D.; Fetters, L. J. *J. Chem. Phys.* **1988**, *89*, 535.
(8) Dudowicz, J.; Freed, K. F.; Lifschitz, M. *Macromolecules* **1994**, *27*, 5387.
(9) Bates, F. S.; Wignall, G. D.; Koehler, W. C. *Phys. Rev. Lett.* **1985**, *55*, 2425.
(10) Bates, F. S.; Wignall, G. D. *Macromolecules* **1986**, *19*, 932.
(11) Jones, R. A. L.; Norton, L. J.; Kramer, E. J.; Bates, F. S.; Wiltzius, P. *Phys. Rev. Lett.* **1991**, *66*, 1326.
(12) Jones, R. A. L.; Kramer, E. J.; Rafailovich, M. H.; Sokolov, J.; Schwarz, S. A. *Phys. Rev. Lett.* **1989**, *62*, 280.
(13) Hariharan, A.; Kumar, S. K.; Rafailovich, M. H.; Sokolov, J.; Zheng, X.; Duong, D. H.; Schwarz, S. A.; Russell, T. P. *J. Chem. Phys.* **1993**, *99*, 656.
(14) Genzer, J.; Composto, R. J. *Polymer* **1999**, *40*, 4223.
(15) Coulon, G.; Russell, T. P.; Deline, V. R.; Green, P. F. *Macromolecules* **1989**, *22*, 2581.
(16) Sferrazza, M.; Xiao, C.; Jones, R. A. L.; Bucknall, D. G.; Webster, J.; Penfold, J. *Phys. Rev.. Lett.* **1997**, *78*, 3693.
(17) Harton, S. E.; Stevie, F. A.; Ade, H. *Macromolecules* **2005**, *38*, 3543.
(18) Fleer, G. J.; Stuart, M. A. C.; Scheutjens, J. M. H. M.; Cosgrove, T.; Vincent, B. *Polymers at Interfaces*; Chapman & Hall: New York, 1993.
(19) Hariharan, A.; Kumar, S. K.; Russell, T. P. *Macromolecules* **1991**, *24*, 4909.
(20) Hariharan, A.; Kumar, S. K.; Russell, T. P. *J. Chem. Phys.* **1993**, *98*, 4163.
(21) Shin, K.; Hu, X.; Zheng, X.; Rafailovich, M. H.; Sokolov, J.; Zaitsev, V.; Schwarz, S. A. *Macromolecules* **2001**, *34*, 4993.
(22) Wilson, R. G.; Stevie, F. A.; Magee, C. W. *Secondary Ion Mass Spectrometry: A Practical Handbook for Depth Profiling and Bulk Impurity Analysis*; John Wiley & Sons: New York, 1989.
(23) Zhao, X.; Zhao, W.; Sokolov, J.; Rafailovich, M. H.; Schwarz, S. A.; Wildens, B. J.; Jones, R. A. L.; Kramer, E. J. *Macromolecules* **1991**, *24*, 5991.
(24) Harton, S. E.; Stevie, F. A.; Ade, H. *Appl. Surf. Sci.*, in press.
(25) Chia, V. K. F.; Mount, G. R.; Edgell, M. J.; Magee, C. W. *J. Vac. Sci. Technol. B* **1999**, *17*, 2345.
(26) Kramer, E. J. *Physica B* **1991**, *173*, 189.
(27) Coleman, M. M.; Narvett, L. A.; Painter, P. C. *Polymer* **1998**, *39*, 5867.
(28) Quirk, R. P.; Yin, J.; Fetters, L. J. *Macromolecules* **1989**, *22*, 85.
(29) Pavlinec, J.; Lazar, M. *J. Appl. Polym. Sci.* **1995**, *55*, 39.
(30) Helfand, E.; Tagami, Y. *J. Polym. Sci., Part B: Polym. Phys.* **1971**, *9*, 741.
(31) Flory, P. J. *Principles of Polymer Chemistry*; Cornell University Press: Ithaca, NY, 1953.
(32) Geoghegan, M.; Nicolai, T.; Penfold, J.; Jones, R. A. L. *Macromolecules* **1997**, *30*, 4220.
(33) Callaghan, T. A.; Paul, D. R. *Macromolecules* **1993**, *26*, 2439.
(34) Postawa, Z.; Czerwinski, B.; Winograd, N.; Garrison, B. J. *J. Phys. Chem. B* **2005**, *109*, 11973.
(35) Russell, T. P.; Karim, A.; Mansour, A.; Felcher, G. P. *Macromolecules* **1988**, *21*, 1890.

(36) Reynolds, B. J.; Ruegg, M. L.; Mates, T. E.; Radke, C. J.; Balsara, N. P. *Macromolecules* **2005**, *38*, 3872.
(37) Antonietti, M.; Coutandin, J.; Sillescu, H. *Makromol. Chem., Rapid Commun.* **1984**, *5*, 525.
(38) Crank, J. *The Mathematics of Diffusion*, 2nd ed.; Oxford University Press: New York, 1975.
(39) Russell, T. P.; Hjelm, R. P.; Seeger, P. A. *Macromolecules* **1990**, *23*, 890.
(40) Wu, S. *J. Phys. Chem.* **1970**, *74*, 632.
(41) Carriere, C. J.; Biresaw, G.; Sammler, R. L. *Rheol. Acta* **2000**, *39*, 476.
(42) Sanchez, I. C.; Lacombe, R. H. *Macromolecules* **1978**, *11*, 1145.
(43) Hariharan, A.; Kumar, S. K.; Russell, T. P. *J. Chem. Phys.* **1993**, *98*, 6516.
(44) Hariharan, A.; Kumar, S. K.; Russell, T. P. *J. Chem. Phys.* **1993**, *99*, 4041.

MA052236Z